Molecular Therapy
Nucleic Acids
Original Article

Cytidine-containing tails robustly enhance and prolong protein production of synthetic mRNA in cell and *in vivo*

Cheuk Yin Li,[1] Zhenghua Liang,[1] Yaxin Hu,[1] Hongxia Zhang,[2] Kharis Daniel Setiasabda,[1] Jiawei Li,[3] Shaohua Ma,[3] Xiaojun Xia,[2] and Yi Kuang[1,4]

[1]Department of Chemical and Biological Engineering, The Hong Kong University of Science and Technology, Clear Water Bay, Kowloon, Hong Kong SAR, China; [2]State Key Laboratory of Oncology in South China, Collaborative Innovation Center for Cancer Medicine, Sun Yat-sen University Cancer Center, Guangzhou, Guangdong 510060, China; [3]Tsinghua-Berkeley Shenzhen Institute, Tsinghua Shenzhen International Graduate School, Tsinghua University, Shenzhen, Guangdong 518057, China; [4]HKUST Shenzhen Research Institute, Shenzhen, Guangdong 518057, China

Synthetic mRNAs are rising rapidly as alternative therapeutic agents for delivery of proteins. However, the practical use of synthetic mRNAs has been restricted by their low cellular stability as well as poor protein production efficiency. The key roles of poly(A) tail on mRNA biology inspire us to explore the optimization of tail sequence to overcome the aforementioned limitations. Here, the systematic substitution of non-A nucleotides in the tails revealed that cytidine-containing tails can substantially enhance the protein production rate and duration of synthetic mRNAs both *in vitro* and *in vivo*. Such C-containing tails shield synthetic mRNAs from deadenylase CCR4-NOT transcription complex, as the catalytic CNOT proteins, especially CNOT6L and CNOT7, have lower efficiency in trimming of cytidine. Consistently, these enhancement effects of C-containing tails were observed on all synthetic mRNAs tested and were independent of transfection reagents and cell types. As the C-containing tails can be used along with other mRNA enhancement technologies to synergically boost protein production, we believe that these tails can be broadly used on synthetic mRNAs to directly promote their clinical applications.

INTRODUCTION

Over the past 2 decades, synthetic mRNAs have been emerging rapidly as new generation of biopharmaceuticals.[1–4] Being able to produce virtually any protein on demand in living cells, synthetic mRNAs harbor broad clinical potentials, among which cellular reprogramming,[5,6] stem cell engineering,[7,8] protein replacement therapy,[1,2,9,10] and mRNA vaccines are highlighted.[2–4] However, several factors have restricted the practical use of synthetic mRNAs, including low cellular stability of mRNA,[10,11] as well as the lack of protein production efficiency.[11,12] To achieve high-performance synthetic mRNAs, several approaches have been implemented: artificial cap analogs[13,14] and optimized untranslated region sequences that enhance translational efficiency of mRNA,[15] modified cytidines and uridines that increase the stability of mRNA,[16,17] etc. Because the poly(A) tail was traditionally considered simply as an adenosine chain, there were limited reports on the optimization of the tail for synthetic mRNAs.[18,19] Recent advanced tail sequencing methods unveiled that more than 10% of human mRNAs possess tails that contain either single or multiple non-adenosine nucleotides, many of which locate at the rear part of the tails.[20–22] However, there has been a lack of thorough examination of the effect of non-adenosine nucleotides in tails in cellular contexts, especially for the tail sequence optimization of synthetic mRNAs.

To address this unmet need, here we investigated the effect of non-adenosine nucleotides in the tail toward the performance of model synthetic mRNAs in cell lines and on mice model. While single G and U substitutions at and near the end of the tail had little or negative impact on protein production from synthetic mRNAs, single C substitution clearly boosted protein production. Further examination revealed that multiple C substitutions near the end of the tail substantially enhanced the protein production rate and extended protein expression time span from mRNAs, with optimal effect achieved with around 20% C substitution. In addition, the C-containing tails also boosted the analyte-sensing performance of two model mRNA switches. Importantly, such C-containing-tail-induced protein production enhancement was consistently observed on all synthetic mRNAs evaluated *in vitro* and *in vivo*. Moreover, the C-containing tail can easily be used together with existing mRNA enhancement techniques to synergically boost the protein production of synthetic mRNAs. Mechanistic studies suggested that the C-containing tails can shield mRNAs from the CNOT complex-induced deadenylation to prolong the intracellular half-life of the mRNA, consequently boosting the protein production. This shielding effect likely stems from the catalytic proteins in the CNOT complex, especially CNOT6L and CNOT7, with lower efficiency in removal of cytidine, thus obstructing the deadenylation process of the CNOT complex.

Received 19 May 2022; accepted 7 October 2022;
https://doi.org/10.1016/j.omtn.2022.10.003.

Correspondence: Yi Kuang, Department of Chemical and Biological Engineering, Hong Kong University of Science and Technology, Hong Kong, Hong Kong.
E-mail: kekuang@ust.hk

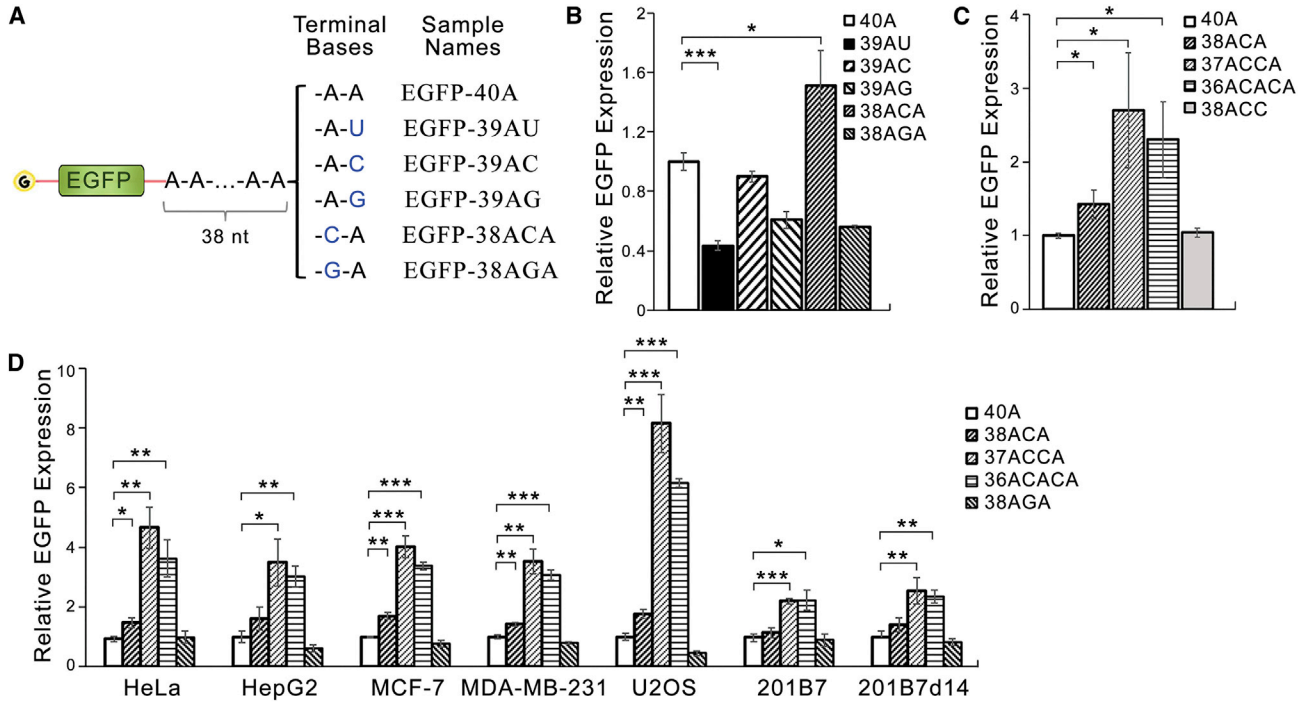

Figure 1. The effect of nucleotide substitution at the end of the tail toward mRNA translation

(A) Scheme showing the EGFP mRNAs with single nucleotide substitution on tail. (B) Relative EGFP expression from HEK293 cells at 24 h post-transfection with single nucleotide substitution on tail. (C) Expression of EGFP from HEK293 cells at 24 h post-transfection with EGFP mRNAs carrying two C substitutions on tail. (D) Relative EGFP expression from various types of human cells at 24 h post-transfection with EGFP mRNAs that carry C substitutions on tail. HeLa: ovarian carcinoma; HepG2: hepatocellular carcinoma, MCF-7: adenocarcinoma, MDA-MB-231: adenocarcinoma, U-2OS: osteosarcoma; 201B7: iPSC; 201B7D14: differentiated 201B7, type nonspecific. n = 3; data are presented as mean ± SD.

The studies in this work set an example of systemic exploration into the tail sequence optimization for synthetic mRNAs, revealing unprecedented C-containing sequences as prominent tails for synthetic mRNAs and implying that natural non-canonical tails may play versatile roles in mRNA biology.

RESULTS

Non-adenosine nucleotides near the end of tail affect protein production of mRNA

Recent tail sequencing of RNAs revealed that more than 10% of human mRNAs have mixed tails,[20–22] among which single and multiple non-A nucleotides exist frequently at the rear part (near or at the 3′ end) of the tails.[20,22] To examine the effect of such non-A nucleotides in the tail on the protein production of mRNAs, we first synthesized a series of EGFP mRNAs with 40-nt tails containing different single nucleotide substitutions at or close to the 3′ end (Figure S1).[23,24] A canonical A-only tail (40A tail) was used as the reference tail. The 40-nt length is sufficient for protein expression of mRNA[25,26] and is within the range of tail length (30A–70A) on synthetic mRNAs in previous reports.[18] The sequences and the names of the tails and the according mRNAs are listed in Figure 1A (see also Table S1). Previous works studying the effect of chemical modifications on protein production enhancement commonly use either the raw fluorescent signals or normalized fluorescent signals for evaluation. To thoroughly present the effect of non-adenosine nucleotide in the tail, the relative EGFP expression calculated based on raw fluorescent signals and the normalized fluorescent signals were analyzed for all experiments.[23] We first observed the raw EGFP expression from HEK293 cells at 4, 24, 48, and 72 h after transfection of the mRNAs using flow cytometry. As shown in Figures S2A and S2B, EGFP-39AU exhibited the lowest EGFP production at all time points, which agreed with previous research that concluded U substitution in the tail favors mRNA degradation.[27] While the other substitutions in the tail either exhibited little effect or caused reduction in protein production, EGFP-38ACA mRNA produced the highest EGFP signals in the cells at all time points (Figure S2A). Analysis of the relative expressions at 24 h post-transfection (the peak of expression of all mRNAs) showed that the enhancement of protein production by EGFP-38ACA is significant (Figure 1B). Similarly, the normalized EGFP expression also revealed enhancement of protein production by the 38ACA tail (Figure S2C). Interestingly, the transfection of EGFP-38ACA induced no-notable cell viability reduction; the transfection of all other mRNAs caused slight cell viability loss (Figure S2D).

To confirm the boosting effect of C substitution on protein production, we then constructed EGFP mRNAs with dual C substitutions

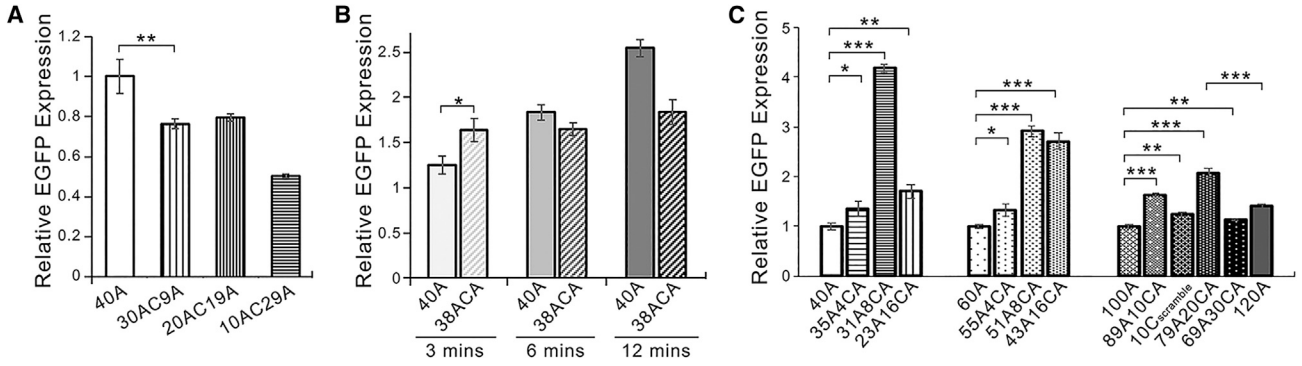

Figure 2. The influence of cytidine location and frequency in the tail toward mRNA translation

(A) Relative EGFP expression from HEK293 cells after transfection with EGFP mRNAs carrying tails with single C substitution at different locations. (B) Relative EGFP expression from HEK293 cells at 24 h post-transfection with EGFP mRNAs carrying 40A or 38ACA tails with additional A residues extended at the 3′ ends by poly(A) polymerase for the indicated durations of time. The results are compared with the EGFP expression from EGFP-40A. (C) Relative EGFP expression from HEK293 cells at 24 h post-transfection with EGFP mRNAs carrying tails of different amount of C substitution. n = 3; data are presented as mean ± SD.

on the tail. Figures 1C and S3A show that the mRNAs with adjacent or separated dual C substitutions near the end of the tail both produced higher amount of EGFP than mRNAs with 40A or 38ACA tails. However, dual C substitution at the end of the tail only induced subtle enhancement of protein production. Thus, in the following experiments, we focused on studying C substitution near the end of the tail. In order to examine whether the effect of C substitution is dependent on cell type, we evaluated mRNAs with dual C-substituted tails on a panel of cell lines that were originated from different human tissues. Besides common immortalized cell lines, human induced pluripotent stem cells 201B7 and its type-nonspecific differentiated cells (denoted as 201B7D14) were included as representatives of stem cells and differentiated somatic cells.[28,29] Even though these cell lines possessed different basal protein expression levels (Figure S3B), EGFP-37ACCA and EGFP-36ACACA produced substantially higher amount of EGFP than EGFP-40A on all cell lines tested (Figures 1D and S3C). Regardless of the difference in the degree of protein expression enhancement across the cell lines, the data clearly stated that the C substitution near the end of the tail can generally induce protein expression enhancement of synthetic mRNA.

Cytidine location and frequency in tail determine the protein production enhancement effect

To examine the influence of C location on the enhancement of protein expression from mRNAs, we constructed EGFP mRNAs with 40-nt tails that contain single C substitution at different locations away from the 3′ end (Table S1). As shown in Figures 2A and S4A, all these mRNAs induced less EGFP expression in HEK293 cells than EGFP-40A, implying that only the C substitution near the end of the tail can enhance protein expression. Because certain translation initiation related poly(A) tail binding proteins (PABP) require continuous A for binding, [30–32] placing C around the center of the 40-nt tail might jeopardize such protein-tail binding, causing bias in the observation. Therefore, we used poly(A) polymerase to extend the 3′ ends of EGFP-40A and EGFP-38ACA with increasing number of A residue by tuning the duration of poly(A) polymerase treatment. All the mRNAs have at least 38 continuous A, of which previous works concluded as sufficient for PABP binding.[30–32] By comparing the protein expression profiles between each pair of the mRNAs on HEK293 cells (Figures 2B and S4B), we found that the C-substitution-induced protein expression enhancement was only preserved in mRNAs with the shortest poly(A) extensions, and it was absent from those with the longer extensions. This result validated the previous observation, confirming that only at locations near the end of the tail can C substitutions enhance protein expression.

On the other hand, to elucidate the relation between C frequency and protein expression enhancement, we designed EGFP mRNAs with 40-nt tails that contain different amounts of C near the end of the tails. Showing on the left of Figure 2C, all the C-containing tails resulted in significantly higher protein expression than EGFP-40A, with EGFP-31A8CA (20% C substitution) exhibiting the highest EGFP production. This experiment was repeated on EGFP mRNAs with 60-nt and 100-nt tails (see also Figures S4C, S4D, S4E, and S4F; Table S1). In the 60-nt tail group, EGFP-51A8CA (13% C substitution) and EGFP-34A16CA (26% C substitution) had similar levels of protein expression enhancement, suggesting the peak of expression can be achieved by tails with C frequency around the middle of this range. In the 100-nt tail group, EGFP-79A20CA (20% C substitution) possessed the highest protein expression. A similar trend between C frequency and translational enhancement was also observed on U2OS cells (Figures S4D and S4F). These results strongly suggested that around 20% C substitution near the end of the tail has optimal protein expression enhancement effect.

Furthermore, as many of the commercial synthetic mRNAs are designed to carry a 120-nt poly(A) tail,[18,33] EGFP-120A was included as a reference mRNA for the EGFP mRNAs with 100-nt tails. Shown in Figures 2C and S4D, the EGFP expression from EGFP-120A was

clearly lower than that from EGFP-79A20CA on both cell lines tested, confirming the enhancement effect of protein expression from C substitution was substantial. Moreover, we found that random substitution of C in the rear part of the tail (EGFP-10$C_{scramble}$ tail; Table S1) also exhibited protein expression enhancement. However, the production level was noticeably lower than that of EGFP-89A10CA (continuous C substitution). Together with the previous result on dual C-substituted tails (Figures 1C and 1D), these data implicated that the continuity of C substitution was a contributing factor toward the protein expression enhancement effect.

Cytidine substitution increases the performance of synthetic mRNA tools

Advanced synthetic mRNA tools, which can sense analyte biomolecules to adjust protein production rate, are gaining increasing attention as tools for cell-specific protein expression controlling.[34–36] To evaluate whether the C-containing tails have an influence on synthetic mRNA tools, we utilized two model mRNA tools: a protein-sensing mRNA switch that senses MS2 coat protein (denoted as MS2CP switch) and a microRNA-sensing mRNA switch that senses microRNA-21-5p (miR-21-5p) (denoted as miR switch),[37,38] both of which can result in expression suppression. In this study, an EGFP ORF was included in both switches as the reporter gene. MS2CP encoding mRNAs at different concentrations was co-transfected with the MS2CP switches to build an intracellular MS2CP concentration gradient. The degree of suppression in EGFP signal (relative fold change) over MS2CP protein gradient represents the sensitivity of the switches toward MS2CP. As shown in Figure 3A, MS2CP switch-79A20CA clearly exhibited stronger MS2CP sensitivity than MS2CP switch-100A. Similarly, we evaluated the performance of the miR switches on identifying HEK293 (low miR-21-5p) and HeLa cells (high miR-21-5p).[39] Shown in Figure S5, the switches with C-containing tails exhibited higher separation fold between the two cells in mix culture (difference in the relative EGFP expression of the two populations), which represented a stronger sensitivity of the switches toward endogenous miR-21-5p. Together, these two data strongly suggested that C-containing tails generally have significant positive influence on the performance of synthetic mRNA tools.

Moreover, antigen-encoding synthetic mRNA is a rising group of safety-optimized prophylactic vaccination.[4] To evaluate the effect of C-containing tails on antigen production, we constructed FLAG-tagged ovalbumin encoding mRNA (denoted as OVA mRNA), a commonly used model mRNA vaccine.[40] As shown in Figure 3B, we used both western blot and flow cytometry to quantify the amount of OVA produced from HEK293 cells transfected with OVA-100A or OVA-79A20CA. Both methods clearly revealed substantially higher OVA production by OVA-79A20CA, suggesting the C-containing tail can also be used to boost antigen production from mRNA vaccine.

As many therapeutic mRNAs encode functional enzymes, we also synthesized model secreted alkaline phosphatase (SEAP) encoding mRNAs (Figure 3C). Every 24 h after transfection, the culture media of HEK293 cells were completely removed for analysis of newly synthesized secretory protein in the media. SEAP-37ACCA and SEAP-31A8CA both produced significantly higher SEAP in the 24-h medium compared with that of SEAP-40A, confirming C-substitution-induced protein expression enhancement. Importantly, SEAP-31A8CA maintained high SEAP production in the 48-h and 72-h media, while little to no SEAP production was observed in the SEAP-40A media (reading below 1 a.u.).[41,42] Similarly, we also examined the effects of the C-containing tails toward firefly luciferase (Luc) mRNAs on HEK293 cells (Figure 3D). The Luc mRNAs carrying C-containing tails clearly produced stronger luminescence at all three time points of observations. These data indicated that C-containing tails not only enhance but also prolong protein production of synthetic mRNA.

Next, we evaluated the effect of the C-containing tails *in vivo*. A polymer-lipid-like material specialized for mRNA vaccine delivery was used to deliver Luc mRNAs with 40A or 31A8CA tails to mice.[40] We observed the peak of protein expression at 6 h after mRNA injection into mice, and the protein expression duration was observed at 24 and 48 h after mRNA injection. As shown in Figures 3E and 3F, the bioluminescence signals on mice injected with Luc-31A8CA were significantly stronger at all three time points. Importantly, Luc-31A8CA at 24 h produced comparable bioluminescence to that of the Luc-40A at 6 h. Also, at 48 h, while the Luc-40A hardly produced any signal, the Luc-31A8CA still produced a certain level of signal. These agreed with the observation on SEAP mRNAs that the C-containing tail can prolong both high protein production window and the overall protein production duration.

Cytidine substitution shields mRNA from CNOT complex-mediated mRNA degradation

As protein production duration is directly correlated with the half-life of the mRNA, we monitored the intracellular amounts of iRFP mRNAs after transfection by qRT-PCR.[43,44] Previous studies reported the average cellular half-lives of synthetic mRNAs to be around 12 h.[16,22,45] Thus, we chose 3, 6, and 12 h after transfection for observation. As shown in Figures 4A and S6A, iRFP-40A showed a clear decrease in amount from 6 to 12 h, while the amount of iRFP-31A8CA was maintained at a nearly similar level. Consequently, a notable difference in production of iRFP from the two mRNAs was observed at 12 h post-transfection (Figure 4B). Moreover, a similar half-life extension was observed also on EGFP mRNAs (Figure S6B). These data suggested that C-containing tail can prolong the intracellular half-life of synthetic mRNA.

Poly(A) tail functions to regulate the degradation of mRNA, while deadenylation, the enzymatic trimming of the tail from the 3′ end, is directly correlated with the decay of mRNAs in cells. It is known that CNOT and PAN2/PAN3 are the two complexes responsible for deadenylation, with PAN2/PAN3 most responsible for trimming long tails (>150 nt) and CNOT for short ones.[46–48] A recent study suggested that PAN2/PAN3 is insensitive to non-A nucleotides, while purified catalytic CNOT proteins exhibit differential deadenylation behaviors against non-A nucleotide-containing oligo RNAs in

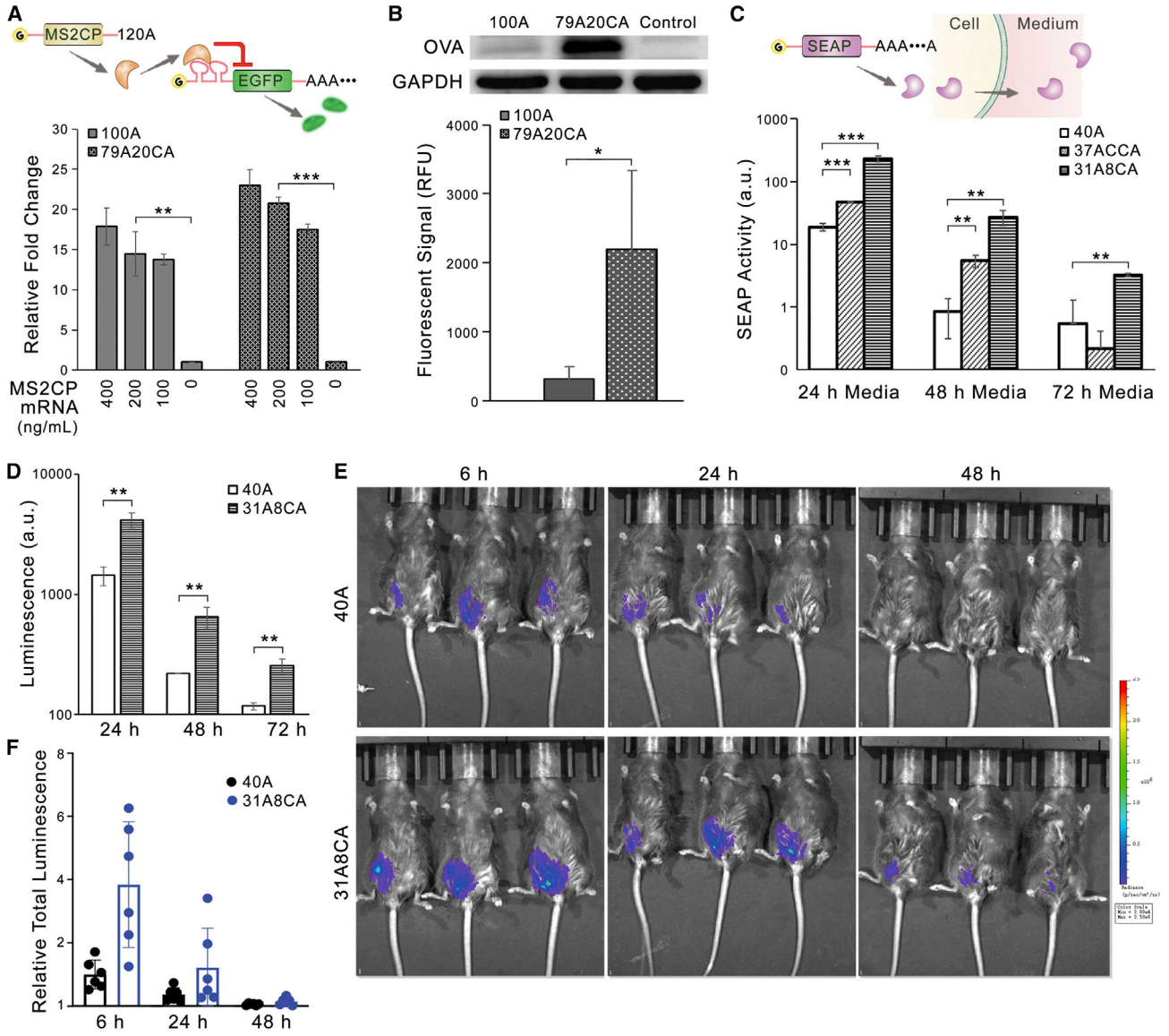

Figure 3. Cytidine substitution on tail enhances the performance of model synthetic mRNAs

(A) Relative expression fold changes from HEK293 at 24 h post-transfection with MS2CP-sensing EGFP-encoding switches with 100A or 79A20CA tail. MS2CP mRNA was co-transfected at different concentrations. (B) Western blot and flow cytometry showing the amount of FLAG-tagged OVA protein after 24 h transfection of OVA mRNA with 100A or 79A20CA tail. (C) SEAP activities in media collected at different time points post-transfection of SEAP mRNAs. After each media collection, fresh media were replaced for continued culture. (D) Luminescence signals from HEK293 cells at 24, 48, and 72 h post-transfection of Luc mRNA with 40A or 31A8CA tails. (E) Representative images showing the bioluminescence signals from mice injected with Luc mRNAs with 40A or 31A8CA tails via subcutaneous injection. (F) Relative total bioluminescence signals recorded from mice injected with the Luc mRNAs. n = 3; data are presented as mean ± SD for panels (A)–(D); n = 6; data are presented as mean ± SD for panel (F).

in vitro deadenylation assay.[49] To evaluate the correlation between C-containing tail and CNOT complex, we applied siRNAs targeting the catalytic CNOT proteins before transfection of EGFP mRNAs. Western blot confirmed that the siRNAs treatment caused partial knockdown of each CNOT protein. (Figures 4C and S6C). Cell viability assay showed that even the transfection of control siRNA significantly affected the cell viability, which could explain the reduced enhancement effect of EGFP expression by the 31A8CA tail in all groups (Figure S6D). As shown in Figure 4D, knockdown of all catalytic CNOT proteins reduced the EGFP expression enhancement by 31A8CA tail, with the effect of CNOT6L and CNOT7 knockdown being significant. Importantly, qRT-PCR showed that the knockdown of CNOT6L and CNOT7 had little effect on changing the cellular amount of EGFP-31A8CA mRNA, while the cellular amount of EGFP-40A increased significantly (Figure 4E). These data strongly implied that CNOT6L and CNOT7 exhibit different

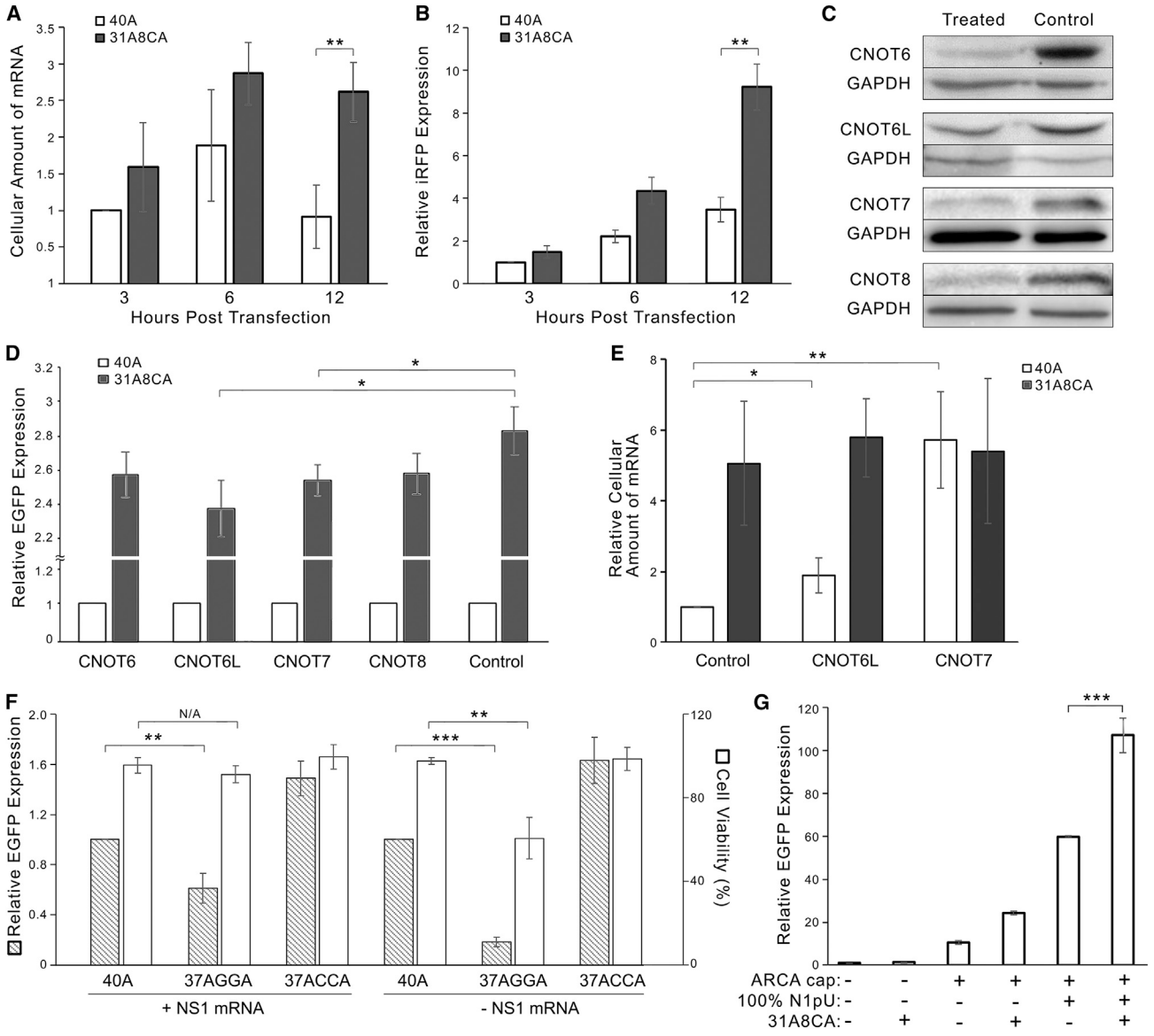

Figure 4. Cytidine substitution on tail prolongs mRNA half-life

(A) qRT-PCR showing the relative intracellular amounts of iRFP mRNAs on HEK293 cells at 3, 6, and 12 h post-transfection. 18S rRNA were used as data normalization. (B) Relative protein expression of iRFP mRNAs on HEK293 cells at 3, 6, and 12 h post-transfection. (C) Western blot showing the amount of CNOT proteins from HEK293 cells treated with according CNOT siRNA (Treated) or control siRNA (Control). GAPDH were used as reference for all samples. (D) Relative EGFP expression on siRNA-treated HEK293 cells at 24 h post-transfection with EGFP-40A or EGFP-31A8CA mRNAs. (E) qRT-PCR showing the relative intracellular amounts of EGFP mRNAs on siRNA-treated HEK293 cells at 12 h post-transfection. 18S rRNA were used as data normalization. (F) Cell viability and relative EGFP expression on HEK293 cells after transfection with EGFP mRNAs with or without pre-transfection of NS1 mRNA. (G) EGFP mRNAs were synthesized to carry cap analog m32.2.7GP3G (−) or ARCA (+); canonical nucleotides (−) or 100% substitution of uridine by *N*1-methylpseudouridine (100% N1pU; +); 40A tail (−) or 31A8CA tail (+). The EGFP mRNAs were transfected to HEK293 cells, and the EGFP expressions were compared with that from EGFP-40A mRNA with m32.2.7GP3G cap and canonical nucleotides. n = 3; data are presented as mean ± SD.

levels of degradation effect toward mRNAs with A-only tail and C tails. Therefore, we believe that the CNOT complex is strongly involved in prolonging the cellular half-life of synthetic mRNA with C-containing tail.

The crystal structure of CNOT6L and poly(A) DNA complex (PDB: 3NGO) suggests that all non-A bases are unfavored for binding with the catalytic pocket of CNOT6L.[50,51] The sequencing data also suggested that cellular mRNAs with C or G in the terminal of the tail

exhibit higher cellular half-lives.[20–22] However, in this study, synthetic mRNAs with G-containing tails showed both repressed protein production and shorter cellular half-lives (Figures S6B and S7A). Unlike cellular mRNAs that are directly produced and used inside the cell, synthetic mRNAs are artificially delivered to cells via transfection. The transfection process is known to affect the performance of synthetic mRNAs, especially if innate immune responses are triggered.[52] As shown in Figure 4F (see also Figures S2B and S7B), transfection of mRNA with G-containing tails induced severe loss of cell viability and reduction of reference iRFP signals. Moreover, pre-transfection of mRNA encoding NS1 protein (influenza A virus, subtype H1N1, strain A/Texas/36/91), a protein that can antagonize the activation of interferon system to reduce transfection-induced innate immune response,[52] was performed 4 h before EGFP mRNA transfection. This treatment fully restored the cell viability and largely restored the protein production of EGFP-37AGGA mRNA. These results indicated that synthetic mRNAs with G in the terminal of the tails might trigger strong innate immune response during transfection, thus exhibiting low protein production rate. On the other hand, mRNA with C-containing tail induced little to no viability loss and consistently showed protein production enhancement with or without NS1 mRNA treatment, allowing higher protein production with even less amount of transfected mRNA (Figure S8A). Together with the fact that the protein production enhancement effect of the C-containing tail is irrelevant to the transfection reagent (Figure S8B), we believe that the C-containing tails do not trigger innate immune response during transfection, so only the C-containing tails can boost synthetic mRNA performance.

At last, as the CNOT complex pathways involved with the C-containing tails are independent of those involved with other mRNA enhancement techniques, such as cap analogs and nucleotide modifications,[13,14,16,17] we evaluated the use of the C-containing tails with these techniques (Figures 4G, S7C, and S8C) and found that synergic effects were observed when both ARCA cap and 31A8CA tails were used, while the strongest protein production was achieved when all three techniques were used. These data strongly suggest that the C-containing tails can work with existing mRNA enhancement techniques to achieve high and stable protein production of synthetic mRNA.

DISCUSSION

The poly(A) tail is a hallmark of mature eukaryotic mRNA, impacting from the nucleus-to-cytosol transportation to the degradation of mRNA. Echoing the recent reports that discovered that non-A nucleotides existed in mouse and human mRNAs, we examined the cellular performance of synthetic mRNAs with tails that contain different non-A nucleotides and furthermore demonstrated the functional roles of non-A nucleotides in mRNA regulation. Our study showcased the power of systematic evaluation of the impact of sequence alteration in the tail to influence protein production and analyte sensitivity from various synthetic mRNAs *in vitro* and *in vivo*.

From the perspective of synthetic mRNA drug development, the findings in this report provided enhanced tail sequences for boosting the efficacy and reducing the dosage of synthetic mRNA therapeutics. We not only identified the optimal location and frequency of C substitution in the tail, but we also demonstrated that the effect of C substitution is general: being independent of encoded protein type, sequence, and length of the overall mRNA, the length of the tail, the type of transfection reagent, as well as the type of transfected cell. While the C substitution alone is sufficient to achieve high protein expression with lower amount of mRNA, the C substitution with modified cap and nucleotides can achieve synergic protein production enhancement. Importantly, the C-containing tails work both *in vitro* and *in vivo*, largely boosting and extending protein production of mRNAs. Therefore, the C-containing tails can broadly promote the applications of existing and future synthetic mRNAs.

Extending from the findings in *in vitro* assay and sequencing works on cellular mRNAs, the work here presented the first piece of cellular experiment on the nucleotide specificity of CNOT6L and CNOT7 toward mRNA degradation. While endogenous mRNAs with G in the tail exhibited prolonged half-lives,[20–22] synthetic mRNAs with G-containing tails induced severe loss of cell viability and low protein production. We believe such difference in observation likely stems from that the synthetic mRNAs with G-containing tails trigger innate immune response during transfection,[52,53] suggesting that the tail sequence may play diverse roles in natural mRNA regulation.

In summary, this work provides prominent C-containing tail sequences that can be readily and generally applied for promoting the performance of a broad spectrum of synthetic mRNAs *in vitro* and *in vivo*. The study highlights the role of C substitution in the rear part of the tail that can shield mRNA from CNOT complex-mediated mRNA degradation and suggests the non-A nucleotides in the tail place versatile roles in the regulation of natural mRNAs.

MATERIALS AND METHODS

Cells lines

All cells were cultured at 37°C with 5% CO_2. All the cells were cultured in recommended growth media and passaged using standard methods. HEK293 cell line was a kind gift of Prof. Pak Hang Peter Cheung, HKUST. HeLa cell line was a kind gift of Prof. Ben Zhong Tang, HKUST. U2OS cell line was a kind gift of Prof. Ben Peng, HKUST. HepG2 cell line was a kind gift of Prof. Randy Poon, HKUST. MDA-MB-231 and MCF-7 cells were purchased from ATCC. hiPSC line 201B7 (201B7),[28] a kind gift from Dr. Hirohide Saito, Kyoto University, was maintained on iMatrix-511 (Nippi, Japan) in complete StemFit (AK02N) medium (Ajinomoto, Japan). Spontaneously differentiated 201B7 (201B7D14) was derived from 201B7 by culturing in StemFit medium without basic FGF for 14 days.[29]

dsDNA template generation

Templates for *in vitro* transcription were generated by fusion PCR using a forward primer that encodes T7 promoter sequence, 5′ UTR fragment, open reading frame fragment, 3′ UTR fragment, and a reverse primer that encodes the reverse complementary of poly(A)

tail sequence. The sequences for poly(A) tail used in this study are reported in Table S1. A $10C_{scramble}$ tail having the same nucleotide frequency as the 89A10CA tail is generated by randomizing the 69^{th}–99^{th} nucleotides (generated by an online tool for scrambled RNA, http://www.sirnawizard.com/scrambled.php). The 5′ UTRs and ORFs sequences have been reported in previously research.[16,39,54] All templates were synthesized using Q5 Hot Start High-Fidelity 2×master mix (NEB, MA, USA). The product templates were purified using QIAquick PCR Purification Kit (Qiagen, Germany). The amounts of templates were determined by NanoVue (GE Healthcare, UK). The purity of templates was assessed using agarose gel electrophoresis. The purity of templates was assessed using agarose gel electrophoresis.

Synthesis and purification of mRNAs

All mRNAs were synthesized using MegaScript T7 Transcription Kit (Thermo Fisher Scientific, MA, USA) with kit-supplied rATP, rCTP, rUTP, 1:4 premix of rGTP, and Anti Reverse Cap Analog (TriLink Biotechnologies, CA, USA). The reaction mixtures were incubated at 37°C for 4 hours and further incubated at 37°C for 30 minutes in the presence of TURBO DNase (Thermo Fisher Scientific, MA, USA). RNA products were purified with an RNA extraction column (Favorgen Biotect, Taiwan) according to the manufacturer's protocol and then subjected to treatment with Antarctic Phosphatase (NEB, MA, USA) at 37°C for 30 minutes. Finally, the product mRNAs were purified again using RNeasy MiniElute Cleanup Kit (Qiagen, Germany). The amounts of product mRNAs were determined by NanoVue (GE Healthcare, UK). The purity of mRNAs was assessed using UREA-PAGE following the standard protocol using 5% gel, stained with GelRed Nucleic Acid Gel Stain (Biotium, CA, USA), and the images were taken by GelDoc Go Imaging System (Bio-Rad, CA, USA). mRNAs were diluted to 100 ng/μL in water and stored at −20°C until use.

Transfection

Cells were seeded into a 24-well plate at 5×10^4 cells/well or 48-well plate at 2.5×10^4 cells/well 1 day prior to the transfection. All test mRNAs and mRNA switches were transfected at a final concentration of 200 ng/mL. For flow cytometry analysis, a reference iRFP mRNA with 120A tail (iRFP-120A) was co-transfected with all EGFP encoding test mRNAs and mRNA switches at a final concentration of 60 ng/mL; a reference EGFP mRNA with 120A tail (EGFP-120A) was co-transfected with iRFP encoding test mRNAs at a final concentration of 60 ng/mL. For protein-sensing mRNA switches, a MS2CP mRNA with 120A tail was co-transfected at gradient concentrations with the switch. Lipofectamine MessengerMAX (Thermo Fisher Scientific, MA, USA) was used to transfect the mRNAs, according to the manufacturer's instructions. For immune evasion study, cells were pre-transfected with 200 ng/mL of NS1-TX91 mRNA 4 h before mRNA transfections.

Poly(A) extension

The procedure follows the manufacturer's protocol. In short, 20-μL reactions were prepared in PCR tubes containing 10 μg of EGFP-40A or EGFP-38ACA mRNA, 1 mM ATP, 1X *E. coli* Poly(A) Polymerase reaction buffer and *E. coli.* Poly(A) Polymerase (NEB, MA, USA) (1 unit; 1 unit can incorporate 1 nmole of AMP into RNA in a 20-μL reaction in 10 min at 37°C). Reaction mixtures were incubated at 37°C for 3, 6, or 12 min to elongate with increasing number of A residues.[55–57] The mixtures were immediately placed on ice after incubation and were purified using RNeasy MiniElute Cleanup Kit (Qiagen, Germany). The amounts of product mRNAs were determined by A_{260} reading on NanoVue (GE Healthcare, UK). The lengths of the mRNAs were analyzed by Fragment Analyzer (Advanced Analytical Technologies, IA, USA).

qRT-PCR

Transfection was performed 24 h after seeding HEK293 cells at 5×10^4 cells/well in a 24-well plate. 200 ng/mL EGFP or iRFP mRNA was transfected into each well. The cell lysate was collected at different time points after the transfection, and total RNA was extracted using Trizol (Thermo Fisher Scientific, MA, USA). 1 μg of total RNA was used to produce cDNA with iScript gDNA Clear cDNA Synthesis Kit (Bio-Rad, CA, USA). The amount of intracellular EGFP mRNA was measured by the standard SYBR Green qRT-PCR protocol and amplification with EGFP, iRFP, and human 18S rRNA-specific primers.[43,44,58] 100 ng of the cDNA was amplified with iTaq Universal SYBR Green Supermix (Bio-Rad, CA, USA) for 40 cycles using CFX96 Real-Time PCR Detection System (Bio-Rad, CA, USA). The Ct values were analyzed with the CFX Manager Software. The Ct value from EGFP mRNA was normalized by the Ct value from 18s rRNA. The data presented show the relative amounts of mRNA calculated by the delta-delta Ct method using the normalized Ct value of EGFP-40A at 1 h after transfection or the normalized Ct value of EGFP-40A from reference siRNA-treated sample as the control.[59]

SEAP activity assay

Cells were seeded into a 24-well plate at 5×10^4 cells/well 1 day prior to transfection. Each SEAP mRNA was transfected at final concentration of 800 ng/mL with Lipofectamine MessengerMAX (Thermo Fisher Scientific, MA, USA) into each well following manufacturer's protocol. The media were collected after 24 h of incubation and stored at −20°C (24 h medium). The cells were immediately rinsed by 1× PBS buffer, then supplied with fresh media and cultured for another 24 h. The media were collected and stored at −20°C (48 h medium). The cells were immediately rinsed by 1×PBS buffer, then supplied with fresh media and cultured for another 24 h. The media were collected and stored at −20°C (72 h medium). The frozen media were thawed and heated at 65°C for 1 h before analysis. The SEAP activity in the media was quantified using Alkaline Phosphatase Activity Fluorometric Assay Kit (Abcam, MA, USA). Background value was measured from media collected from cells transfected with only Lipofectamine MessengerMAX. The background value was subtracted from all other readings in analysis.

Luciferase assay

HEK293 cells were seeded in 96-well plates at density of 2×10^4 cells per well, 24 h after transfection with Luc mRNA, 100 μL D-Luciferin

(Thermo Fisher Scientific, MA, USA) was added to each well to a final concentration of 150 μg/mL. After 5 min, the luminescence intensities were measured by Varioskan LUX multimode microplate reader (Thermo Fisher Scientific, MA, USA).

Western blot

Cells were lysed with CelLytic M Cell Lysis Reagent (Sigma-Aldrich, MA, USA), supplemented with protease inhibitor (Thermo Fisher Scientific, MA, USA) on ice for 15 min, and clarified by centrifugation. The protein concentration was measured by BCA assay (Thermo Fisher Scientific, MA, USA). An equal amount of total protein extract (~20 μg) was separated by 12% sodium dodecyl sulfate polyacrylamide gel electrophoresis (SDS-PAGE). The samples were transferred to methanol-activated polyvinylidene fluoride (PVDF) membranes (Bio-Rad, CA, USA) using semi-dry transfer method by Trans-Blot Turbo Transfer System (Bio-Rad, CA, USA). The membrane was blocked with 1× PBST containing 5% skim milk for 1 h at room temperature, then incubated with primary antibody at 4°C overnight. On the second day, the membrane was washed with 1× PBST five times and incubated with the secondary antibody for 1 h at room temperature. The protein was detected with ECL Western Blotting Reagent and ChemiDoc XRS. After imaging of the target protein stain, the membranes were washed twice by stripping buffer (1% Tween 20, 0.1% SDS, pH 2.2 in distilled water) and then washed three times by 1× PBST containing 5% skim milk. The membranes were then stained for GAPDH following the above procedures. The images were analyzed with ImageJ and Image Lab software (Bio-Rad, CA, USA). Rabbit Anti-DDDDK tag antibody (Abcam, CAT# ab245892, MA, USA) was used in 1:500 dilution. Rabbit anti-GAPDH antibody (Novus Biologicals, CO, USA; CAT# NB100-56875) was used in 1:2,000 dilution. Rabbit anti-CNOT6 (Novus Biologicals, CO, USA; CAT# NBP1-57550) was used in 1:500 dilution. Rabbit anti-CNOT6L (Sigma-Aldrich, MA, USA; CAT# SAB1303263) was used in 1:1,000 dilution. Rabbit anti-CNOT7 (Novus Biologicals, CO, USA; CAT# NBP2-92571) was used in 1:500 dilution. CNOT8 (Novus Biologicals, CO, USA; CAT# NBP2-15930) was used in 1:500 dilution. HRP conjugated goat anti-rabbit antibody (Novus Biologicals, CO, USA; CAT# NB7160) was used in 1:2,000 dilution.

In vivo bioluminescence

6- to 8-week-old female C57BL/6J mice (Vital River Laboratory) were maintained under specific-pathogen-free conditions and were kept with a 12-h/12-h light/dark cycle in individually ventilated cages, provided with food and water *ad libitum*. All animal procedures were approved and controlled by the local ethics committee and carried out according to the guidelines of protection of animal life. The animals were injected subcutaneously with 10 μg mRNA encapsulated with polymer-lipid-like material C1.[40] In brief, lipid-like material C1 and synthesized mRNA in aqueous solution were mixed at a weight ratio of 160:1 to form C1-mRNA complex. And then, DSPE-PEG2000 was added followed by vortex mixing at a weight ratio of 1:5 to C1. At 6, 24, and 48 h after mRNA injection, the mice were anesthetized intraperitoneally with 5% chloral hydrate (150 μL/mouse) and injected intraperitoneally with D-Luciferin solution (150 mg/kg mice). The bioluminescence images of the mice were taken 15 min after D-Luciferin injection on IVIS. The total bioluminescence signals of the lower right abdomen were recorded for calculation.

siRNA transfection

The sequences of the siRNAs targeting CNOT6, CNOT6L, CNOT7, and CNOT8 are as described in the literature.[60] siGENOME non-targeting siRNA Control Pools (Horizon, UK) were used as reference siRNAs. All siRNAs (RIBOBIO, China) were transfected to HEK293 cells at final concentration of 50 nM using DharmaFECT Transfection reagent (Horizon, UK) following manufacturer's protocol. After 48 h of siRNA transfection, the cells were trypsinized and seeded at 2.5×10^4 cells per well in a 48-well plate. 24 h after seeding, the cells were transfected with EGFP mRNAs with different tails following the above-described procedure.

Flow cytometry analysis

All cell samples were analyzed by Attune NxT Flow Cytometry (Thermo Fisher Scientific, MA, USA) and BD FACSAria III (BD biosciences, NJ, USA). The flow cytometry was calibrated with Attune Performance Tracking Beads (Thermo Fisher Scientific, MA, USA) or BD FACSDiva CS&T Research Beads (BD biosciences, NJ, USA) following manufacturer's recommendation before every experiment. After desired hours of mRNA transfection, the cells were suspended using 0.25% trypsin. The cell suspensions were diluted in PBS buffer with 10% FBS and then passed through a 35-micron nylon mesh. EGFP/Alexa Fluor 488 signals were detected by excitation laser at 488 nm and emission filter at 530/30 nm. iRFP signals were detected by excitation laser at 637 nm and emission filter at 670/14 nm. Dead cells and debris were removed by front and lateral light scattering signals, and doublet discrimination was performed by area and height of front scattering signals.[61] A negative control sample transfected with only the Lipofectamine MessengerMAX was used to gate for viable cell population. The relative viabilities of the other samples were calculated by comparing the viable cell number to that of the negative control sample. The iRFP intensities from the viable cell populations were used to gate for the positively transfected cell population. For relative EGFP expression, the EGFP intensities from the positively transfected cell populations were recorded and compared with the intensities from EGFP mRNAs carrying A-only tails. For the normalized EGFP expression, the EGFP intensities from the positively transfected cell populations were normalized by the iRFP intensities. For cells transfected with mRNA switches, the EGFP intensities were first normalized by the iRFP intensities to generate the adjusted EGFP expression before further analysis, following the procedure of previous research.[39] To evaluate the expression of ovalbumin tagged with FLAG, cell suspensions were first incubated with 0.4% formaldehyde for 20 min. After washing with 1× PBS (1% BSA) twice, the cells were permeabilized with 0.1% Triton X-100 for 10 min. After washing twice, the cells were stained with Recombinant Alexa Fluor 488 Anti-DDDDK tag antibody (Abcam, MA, USA) for 1 h at room temperature. After washing thrice, the stained cells were analyzed by flow cytometry.

The positively transfected cells were gated by iRFP intensities, and the Fluor 488 intensities of the positively transfected populations were recorded for analysis.

Quantification and statistical analysis

Statistical values including the exact N and statistical significance are reported in the figure legends. Standard deviation was calculated using Excel. Significant differences were determined using one-way ANOVA. The statistical analysis is based on the means generated from at least three independent experiments, unless specified otherwise. Dot plots and histograms were produced from Invitrogen Attune NxT flow cytometry software. The levels of significance are denoted as *$p < 0.05$, **$p < 0.01$, ***$p < 0.001$.

DATA AVAILABILITY

The data for this study are available from the authors upon request.

SUPPLEMENTAL INFORMATION

Supplemental information can be found online at https://doi.org/10.1016/j.omtn.2022.10.003.

ACKNOWLEDGMENTS

We appreciate Prof. Hirohide Saito for providing us with the plasmids of EGFP, iRFP, and PALP as well as the 201B7 cell line. We thank Prof. Pak Hang Peter Cheung for HEK 293 cell line, Prof. Ben Zhong Tang for HeLa cell line, Prof. Ben Peng for U2OS cell line, and Prof. Randy Poon for HepG2 cell line. The work is supported by Early Career Scheme from Research Grants Council of Hong Kong (26308419), Bridge Gap Fund by HKUST (BGI.016.2021), and Chau Hoi Shuen Foundation (Z0579).

AUTHOR CONTRIBUTIONS

Y.K. and C.Y.L. designed the research. C.Y.L. executed the experiments and analyzed the result. Z.L., Y.H., and K.D.S. assisted with the data collection and validated the result. H.Z. executed the *in vivo* experiments and assisted with the OVA expression experiments. J. L. and M.S. assisted with RNA characterization and data curation. X.X. coordinated the OVA expression experiments and supervised the *in vivo* experiments. Y.K. and C.Y.L. wrote the manuscript. Y.K. coordinated and supervised the project. All authors have read and approved the manuscript and its content.

DECLARATION OF INTERESTS

All authors hereby declare no conflict of interest relating to this manuscript.

REFERENCES

1. Sahin, U., Karikó, K., and Türeci, Ö. (2014). mRNA-based therapeutics — developing a new class of drugs. Nat. Rev. Drug Discov. *13*, 759–780.
2. Kowalski, P.S., Rudra, A., Miao, L., and Anderson, D.G. (2019). Delivering the messenger: advances in technologies for therapeutic mRNA delivery. Mol. Ther. *27*, 710–728.
3. Pascolo, S. (2008). Vaccination with messenger RNA (mRNA). In Toll-Like Receptors (TLRs) and Innate Immunity, S. Bauer and G. Hartmann, eds., pp. 221–235.
4. Pardi, N., Hogan, M.J., Porter, F.W., and Weissman, D. (2018). mRNA vaccines — a new era in vaccinology. Nat. Rev. Drug Discov. *17*, 261–279.
5. Artero Castro, A., León, M., Del Buey Furió, V., Erceg, S., and Lukovic, D. (2018). Generation of a human iPSC line by mRNA reprogramming. Stem Cell Res. *28*, 157–160.
6. Warren, L., and Lin, C. (2019). mRNA-based genetic reprogramming. Mol. Ther. *27*, 729–734.
7. Warren, L., Manos, P.D., Ahfeldt, T., Loh, Y.-H., Li, H., Lau, F., Ebina, W., Mandal, P.K., Smith, Z.D., Meissner, A., et al. (2010). Highly efficient reprogramming to pluripotency and directed differentiation of human cells with synthetic modified mRNA. Cell Stem Cell *7*, 618–630.
8. Steinle, H., Behring, A., Schlensak, C., Wendel, H.P., and Avci-Adali, M. (2017). Concise review: application of in vitro transcribed messenger RNA for cellular engineering and reprogramming: progress and challenges. Stem Cell. *35*, 68–79.
9. Vallazza, B., Petri, S., Poleganov, M.A., Eberle, F., Kuhn, A.N., and Sahin, U. (2015). Recombinant messenger RNA technology and its application in cancer immunotherapy, transcript replacement therapies, pluripotent stem cell induction, and beyond. Wiley Interdiscip. Rev. RNA *6*, 471–499.
10. Kwon, H., Kim, M., Seo, Y., Moon, Y.S., Lee, H.J., Lee, K., and Lee, H. (2018). Emergence of synthetic mRNA: in vitro synthesis of mRNA and its applications in regenerative medicine. Biomaterials *156*, 172–193.
11. Van Tendeloo, V.F.I., Ponsaerts, P., and Berneman, Z.N. (2007). mRNA-based gene transfer as a tool for gene and cell therapy. Curr. Opin. Mol. Ther. *9*, 423–431.
12. Suknuntha, K., Tao, L., Brok-Volchanskaya, V., D'Souza, S.S., Kumar, A., and Slukvin, I. (2018). Optimization of synthetic mRNA for highly efficient translation and its application in the generation of endothelial and hematopoietic cells from human and primate pluripotent Stem Cells. Stem Cell Rev. Rep. *14*, 525–534.
13. Kocmik, I., Piecyk, K., Rudzinska, M., Niedzwiecka, A., Darzynkiewicz, E., Grzela, R., and Jankowska-Anyszka, M. (2018). Modified ARCA analogs providing enhanced translational properties of capped mRNAs. Cell Cycle *17*, 1624–1636.
14. Wojtczak, B.A., Sikorski, P.J., Fac-Dabrowska, K., Nowicka, A., Warminski, M., Kubacka, D., Nowak, E., Nowotny, M., Kowalska, J., and Jemielity, J. (2018). 5'-phosphorothiolate dinucleotide cap analogues: reagents for messenger RNA modification and potent small-molecular inhibitors of decapping enzymes. J. Am. Chem. Soc. *140*, 5987–5999.
15. Asrani, K.H., Farelli, J.D., Stahley, M.R., Miller, R.L., Cheng, C.J., Subramanian, R.R., and Brown, J.M. (2018). Optimization of mRNA untranslated regions for improved expression of therapeutic mRNA. RNA Biol. *15*, 756–762.
16. Parr, C.J.C., Wada, S., Kotake, K., Kameda, S., Matsuura, S., Sakashita, S., Park, S., Sugiyama, H., Kuang, Y., and Saito, H. (2020). N1-Methylpseudouridine substitution enhances the performance of synthetic mRNA switches in cells. Nucleic Acids Res. *48*, e35.
17. Uchida, S., Kataoka, K., and Itaka, K. (2015). Screening of mRNA chemical modification to maximize protein expression with reduced immunogenicity. Pharmaceutics *7*, 137–151.
18. Holtkamp, S., Kreiter, S., Selmi, A., Simon, P., Koslowski, M., Huber, C., Türeci, O., and Sahin, U. (2006). Modification of antigen-encoding RNA increases stability, translational efficacy, and T-cell stimulatory capacity of dendritic cells. Blood *108*, 4009–4017.
19. Strzelecka, D., Smietanski, M., Sikorski, P.J., Warminski, M., Kowalska, J., and Jemielity, J. (2020). Phosphodiester modifications in mRNA poly(A) tail prevent deadenylation without compromising protein expression. RNA *26*, 1815–1837.
20. Legnini, I., Alles, J., Karaiskos, N., Ayoub, S., and Rajewsky, N. (2019). FLAM-seq: full-length mRNA sequencing reveals principles of poly(A) tail length control. Nat. Methods *16*, 879–886.
21. Lim, J., Kim, D., Lee, Y.S., Ha, M., Lee, M., Yeo, J., Chang, H., Song, J., Ahn, K., and Kim, V.N. (2018). Mixed tailing by TENT4A and TENT4B shields mRNA from rapid deadenylation. Science *361*, 701–704.
22. Chang, H., Lim, J., Ha, M., and Kim, V.N. (2014). TAIL-seq: genome-wide determination of poly(A) tail length and 3′ end modifications. Mol. Cell *53*, 1044–1052.

23. Moradian, H., Roch, T., Anthofer, L., Lendlein, A., and Gossen, M. (2022). Chemical modification of uridine modulates mRNA-mediated proinflammatory and antiviral response in primary human macrophages. Mol. Ther. Nucleic Acids *27*, 854–869.

24. Baiersdörfer, M., Boros, G., Muramatsu, H., Mahiny, A., Vlatkovic, I., Sahin, U., and Karikó, K. (2019). A facile method for the removal of dsRNA contaminant from in vitro-transcribed mRNA. Mol. Ther. Nucleic Acids *15*, 26–35.

25. Peng, J., and Schoenberg, D.R. (2005). mRNA with a <20-nt poly(A) tail imparted by the poly(A)-limiting element is translated as efficiently in vivo as long poly(A) mRNA. RNA *11*, 1131–1140.

26. Hajj, K.A., and Whitehead, K.A. (2017). Tools for translation: non-viral materials for therapeutic mRNA delivery. Nat. Rev. Mater. *2*, 17056.

27. Lim, J., Ha, M., Chang, H., Kwon, S.C., Simanshu, D.K., Patel, D.J., and Kim, V.N. (2014). Uridylation by TUT4 and TUT7 marks mRNA for degradation. Cell *159*, 1365–1376.

28. Takahashi, K., Tanabe, K., Ohnuki, M., Narita, M., Ichisaka, T., Tomoda, K., and Yamanaka, S. (2007). Induction of pluripotent stem cells from adult human fibroblasts by defined factors. Cell *131*, 861–872.

29. Nakagawa, M., Taniguchi, Y., Senda, S., Takizawa, N., Ichisaka, T., Asano, K., Morizane, A., Doi, D., Takahashi, J., Nishizawa, M., et al. (2014). A novel efficient feeder-free culture system for the derivation of human induced pluripotent stem cells. Sci. Rep. *4*, 3594.

30. Sawazaki, R., Imai, S., Yokogawa, M., Hosoda, N., Hoshino, S.I., Mio, M., Mio, K., Shimada, I., and Osawa, M. (2018). Characterization of the multimeric structure of poly(A)-binding protein on a poly(A) tail. Sci. Rep. *8*, 1455.

31. Kühn, U., Nemeth, A., Meyer, S., and Wahle, E. (2003). The RNA binding domains of the nuclear poly(A)-binding protein. J. Biol. Chem. *278*, 16916–16925.

32. Deo, R.C., Bonanno, J.B., Sonenberg, N., and Burley, S.K. (1999). Recognition of polyadenylate RNA by the poly(A)-binding protein. Cell *98*, 835–845.

33. Oh, S., and Kessler, J.A. (2018). Design, assembly, production, and transfection of synthetic modified mRNA. Methods *133*, 29–43.

34. Kawasaki, S., Fujita, Y., Nagaike, T., Tomita, K., and Saito, H. (2017). Synthetic mRNA devices that detect endogenous proteins and distinguish mammalian cells. Nucleic Acids Res. *45*, e117.

35. Ohno, H., Akamine, S., and Saito, H. (2020). Synthetic mRNA-based systems in mammalian cells. Adv. Biosyst. *4*, 1900247.

36. Wieland, M., and Hartig, J.S. (2008). Artificial riboswitches: synthetic mRNA-based regulators of gene expression. Chembiochem *9*, 1873–1878.

37. Wroblewska, L., Kitada, T., Endo, K., Siciliano, V., Stillo, B., Saito, H., and Weiss, R. (2015). Mammalian synthetic circuits with RNA binding proteins for RNA-only delivery. Nat. Biotechnol. *33*, 839–841.

38. Miki, K., Endo, K., Takahashi, S., Funakoshi, S., Takei, I., Katayama, S., Toyoda, T., Kotaka, M., Takaki, T., Umeda, M., et al. (2015). Efficient detection and purification of cell populations using synthetic microRNA switches. Cell Stem Cell *16*, 699–711.

39. Matsuura, S., Ono, H., Kawasaki, S., Kuang, Y., Fujita, Y., and Saito, H. (2019). Synthetic RNA-based logic computation in mammalian cells. Nat. Commun. *10*, 1950.

40. Zhang, H., You, X., Wang, X., Cui, L., Wang, Z., Xu, F., Li, M., Yang, Z., Liu, J., Huang, P., et al. (2021). Delivery of mRNA vaccine with a lipid-like material potentiates antitumor efficacy through Toll-like receptor 4 signaling. Proc. Natl. Acad. Sci. USA *118*, e2005191118.

41. Schrenkhammer, P., Rosnizeck, I.C., Duerkop, A., Wolfbeis, O.S., and Schäferling, M. (2008). Time-resolved fluorescence-based assay for the determination of alkaline phosphatase activity and application to the screening of its inhibitors. J. Biomol. Screen *13*, 9–16.

42. Obayashi, Y., Iino, R., and Noji, H. (2015). A single-molecule digital enzyme assay using alkaline phosphatase with a cumarin-based fluorogenic substrate. Analyst *140*, 5065–5073.

43. Nygard, A.B., Jørgensen, C.B., Cirera, S., and Fredholm, M. (2007). Selection of reference genes for gene expression studies in pig tissues using SYBR green qPCR. BMC Mol. Biol. *8*, 67.

44. Cao, H., and Shockey, J.M. (2012). Comparison of TaqMan and SYBR Green qPCR methods for quantitative gene expression in tung tree tissues. J. Agric. Food Chem. *60*, 12296–12303.

45. Schwanhäusser, B., Busse, D., Li, N., Dittmar, G., Schuchhardt, J., Wolf, J., Chen, W., and Selbach, M. (2011). Global quantification of mammalian gene expression control. Nature *473*, 337–342.

46. Chen, C.Y.A., Zhang, Y., Xiang, Y., Han, L., Chang, J.T., and Shyu, A.B. (2017). Antagonistic actions of two human Pan3 isoforms on global mRNA turnover. RNA *23*, 1404–1418.

47. Yi, H., Park, J., Ha, M., Lim, J., Chang, H., and Kim, V.N. (2018). PABP cooperates with the CCR4-NOT complex to promote mRNA deadenylation and block precocious decay. Mol. Cell *70*, 1081–1088.e5.

48. Tudek, A., Krawczyk, P.S., Mroczek, S., Tomecki, R., Turtola, M., Matylla-Kulińska, K., Jensen, T.H., and Dziembowski, A. (2021). Global view on the metabolism of RNA poly (A) tails in yeast Saccharomyces cerevisiae. Nat. Commun. *12*, 4951.

49. Tang, T.T.L., Stowell, J.A.W., Hill, C.H., and Passmore, L.A. (2019). The intrinsic structure of poly(A) RNA determines the specificity of Pan2 and Caf1 deadenylases. Nat. Struct. Mol. Biol. *26*, 433–442.

50. Wang, H., Morita, M., Yang, X., Suzuki, T., Yang, W., Wang, J., Ito, K., Wang, Q., Zhao, C., Bartlam, M., et al. (2010). Crystal structure of the human CNOT6L nuclease domain reveals strict poly(A) substrate specificity. EMBO J. *29*, 2566–2576.

51. Chen, Y., Khazina, E., Izaurralde, E., and Weichenrieder, O. (2021). Crystal structure and functional properties of the human CCR4-CAF1 deadenylase complex. Nucleic Acids Res. *49*, 6489–6510.

52. Liu, Y., Chin, J.M., Choo, E.L., and Phua, K.K.L. (2019). Messenger RNA translation enhancement by immune evasion proteins: a comparative study between EKB (vaccinia virus) and NS1 (influenza A virus). Sci. Rep. *9*, 11972.

53. Kim, D., Lee, Y.S., Jung, S.-J., Yeo, J., Seo, J.J., Lee, Y.-Y., Lim, J., Chang, H., Song, J., Yang, J., et al. (2020). Viral hijacking of the TENT4–ZCCHC14 complex protects viral RNAs via mixed tailing. Nat. Struct. Mol. Biol. *27*, 581–588.

54. Parr, C.J.C., Katayama, S., Miki, K., Kuang, Y., Yoshida, Y., Morizane, A., Takahashi, J., Yamanaka, S., and Saito, H. (2016). MicroRNA-302 switch to identify and eliminate undifferentiated human pluripotent stem cells. Sci. Rep. *6*, 32532.

55. Flanegan, J.B., and Baltimore, D. (1977). Poliovirus-specific primer-dependent RNA polymerase able to copy poly(A). Proc. Natl. Acad. Sci. USA *74*, 3677–3680.

56. Kerwitz, Y., Kühn, U., Lilie, H., Knoth, A., Scheuermann, T., Friedrich, H., Schwarz, E., and Wahle, E. (2003). Stimulation of poly(A) polymerase through a direct interaction with the nuclear poly(A) binding protein allosterically regulated by RNA. EMBO J. *22*, 3705–3714.

57. Wahle, E. (1995). Poly(A) tail length control is caused by termination of processive synthesis. J. Biol. Chem. *270*, 2800–2808.

58. Radonić, A., Thulke, S., Mackay, I.M., Landt, O., Siegert, W., and Nitsche, A. (2004). Guideline to reference gene selection for quantitative real-time PCR. Biochem. Biophys. Res. Commun. *313*, 856–862.

59. Vandesompele, J., De Preter, K., Pattyn, F., Poppe, B., Van Roy, N., De Paepe, A., and Speleman, F. (2002). Accurate normalization of real-time quantitative RT-PCR data by geometric averaging of multiple internal control genes. Genome Biol. *3*. RESEARCH0034.

60. Ito, K., Takahashi, A., Morita, M., Suzuki, T., and Yamamoto, T. (2011). The role of the CNOT1 subunit of the CCR4-NOT complex in mRNA deadenylation and cell viability. Protein Cell *2*, 755–763.

61. Wersto, R.P., Chrest, F.J., Leary, J.F., Morris, C., Stetler-Stevenson, M.A., and Gabrielson, E. (2001). Doublet discrimination in DNA cell-cycle analysis. Cytometry *46*, 296–306.